

## How Noise and Coupling Induce Bursting Action Potentials in Pancreatic $\beta$ -cells

Junghyo Jo,<sup>\*</sup> Hyuk Kang,<sup>\*</sup> Moo Young Choi,<sup>\*†</sup> and Duk-Su Koh<sup>‡</sup>

<sup>\*</sup>Department of Physics, Seoul National University, Seoul 151-747, Korea;

<sup>†</sup>Korea Institute for Advanced Study, Seoul 130-722, Korea; and <sup>‡</sup>Department of Physics, Pohang University of Science and Technology, Pohang 790-784, Korea

E-mail: mychoi@snu.ac.kr

Corresponding author's present address: Department of Physics, Seoul National University, Seoul 151-747, Korea; and Korea Institute for Advanced Study, Seoul 130-722, Korea

## **Abstract**

Unlike isolated  $\beta$ -cells, which usually produce continuous spikes or fast and irregular bursts, electrically coupled  $\beta$ -cells are apt to exhibit robust bursting action potentials. We consider the noise induced by thermal fluctuations as well as that by channel gating stochasticity and examine its effects on the action potential behavior of the  $\beta$ -cell model. It is observed numerically that such noise in general helps single cells to produce a variety of electrical activities. In addition, we also probe coupling via gap junctions between neighboring cells, with heterogeneity induced by noise, to find that it enhances regular bursts.

*Key words:* Thermal fluctuation; Channel gating stochasticity; Heterogeneity; Gap junction

## **Introduction**

Bursting action potentials, which are characterized by rapid firing interspersed with quiescent periods in pancreatic  $\beta$ -cells, play a central role in the secretion of insulin, the hormone for glucose homeostasis. It has been reported that isolated  $\beta$ -cells actually show continuous spikes or fast and irregular bursts (1, 2, 3) while  $\beta$ -cells in a cluster or in an intact islet produce regular bursting action potentials (4, 5, 6, 7). As for the correlations between the electrical activity on the cell membrane and insulin secretion (8), the robust bursts appear more effective in maintaining glucose homeostasis than continuous spikes, since coupled  $\beta$ -cells can control insulin release better than isolated  $\beta$ -cells (9, 10, 11).

However, the question as to whether bursting is an endogenous property of individual  $\beta$ -cells or of a cluster still remains to be answered, which has attracted a number of investigations. Among proposed explanations is the channel-sharing hypothesis, which postulates that current fluctuations arising from channel gating stochasticity prevent single cells, originally capable of bursting, from bursting, but when they are electrically coupled, the perturbing effects are shared by neighbors and the regular bursting is recovered (12, 13, 14). In contrast to this hypothesis of negative effects of noise, recent research (15, 16, 17, 18, 19) has established that noise can play a constructive role in many biological systems including  $\beta$ -cell bursting (20). The heterogeneity hypothesis, providing another explanation, was also postulated by the same group. According to it, when heterogeneous cells, each of which produces continuous spikes or bursts depending upon such cell

parameters as the size, channel density, etc., are coupled, those cells in the cluster exhibit more pronounced bursts. This gives a useful insight into the functioning of heterogeneous cell populations (21).

In this study, we expand the concept of heterogeneity and probe how such general heterogeneity enhances bursting. It is proposed that noise induces heterogeneity in otherwise homogeneous individual  $\beta$ -cells, which in turn assists the  $\beta$ -cells to produce robust bursts when they are coupled. Existing studies have mostly focused on the synchronizing role of coupling (22, 23); the slow dynamics, which has a period about 10 to 60 seconds, is synchronized successfully between adjacent cells. In contrast, we focus here on the fact that rapid firing in the active phase of bursting is asynchronous between neighbors (24) and these fluctuating currents through the gap junction act like noise, enhancing the robust bursting action potential. It is also presented that various action potentials of single  $\beta$ -cells are embodied with optimal noise induced by thermal fluctuations or by ionic channel gating stochasticity. In particular, noise stimulates occasionally itself to produce *fast bursts* in a single cell.

There are four sections in this paper: In the second section the mathematical model for  $\beta$ -cells is introduced and the simulation method is described. The third section is devoted to the effects of random noise in currents and of voltage-dependent noise in single cells while the fourth section examines how coupling between cells influences the electrical activity of a cell. Finally, main results are summarized and discussed in the last section.

## Model and Methods

### Mathematical model for a $\beta$ -cell

As the Hodgkin-Huxley model (25) describes the electrical activity on the cell membrane with ion channels, a few mathematical models for  $\beta$ -cells, based on the electrophysiological data (26, 27, 28) of the ion channels in  $\beta$ -cells, have been proposed. Although there are simple models using two-dimensional maps (29, 30, 31), we consider the Sherman model, which allows direct physical interpretation (20, 32).

The model is described by the current balance equation between capacitive and ionic currents:

$$C_M \frac{dV}{dt} = -I_{Ca}(V) - I_K(V, N) - I_{K(ATP)}(V, P) - I_S(V, S), \quad (1)$$

where  $C_M$  and  $V$  denote the membrane capacitance and the membrane potential, respectively. The activation variable  $N$  and the slow variable  $S$  are governed by

$$\begin{aligned} \tau_N \frac{dN}{dt} &= N_\infty(V) - N \\ \tau_S \frac{dS}{dt} &= S_\infty(V) - S \end{aligned} \quad (2)$$

with appropriate relaxation times  $\tau_N$  and  $\tau_S$ , which are taken to be constants for simplicity. The fraction  $P$  of open K(ATP) channels may also be regarded as a constant for the moment [see Eq. 11]. Ionic currents here are fast

voltage-dependent L-type  $\text{Ca}^{2+}$  current  $I_{Ca}$ , delayed-rectifier  $\text{K}^+$  current  $I_K$ , ATP-blockable  $\text{K}^+$  current  $I_{K(ATP)}$ , and very slow inhibitory potassium current  $I_S$ :

$$\begin{aligned}
 I_{Ca}(V) &= g_{Ca}M_\infty(V)(V - V_{Ca}) \\
 I_K(V, N) &= g_K N(V - V_K) \\
 I_{K(ATP)}(V, P) &= g_{K(ATP)}P(V - V_K) \\
 I_S(V, S) &= g_S S(V - V_K).
 \end{aligned} \tag{3}$$

$I_{Ca}$  and  $I_K$  are responsible for generating action potentials;  $I_{Ca}$  is assumed to respond instantaneously to a change in the membrane potential, whereas  $I_K$  is governed by the dynamics of the activation variable  $N$  via Eq. 2.  $I_{K(ATP)}$  is the background current with voltage-independent conductance  $g_{K(ATP)}$ ; this determines the plateau fraction, i.e., the ratio of the active phase duration to the burst period. For example, as  $g_{K(ATP)}$  decreases under high glucose concentration, there are only active phases without silent phases.  $I_S$  is a phenomenological current representing slow dynamics in the bursting action potential. This model thus assumes that single  $\beta$ -cells originally contain the slow dynamics, which works just under the appropriate condition. Biological candidates for such slow dynamics include slow free  $\text{Ca}^{2+}$  dynamics (33) and ATP metabolism (34). Finally,  $M_\infty$ ,  $N_\infty$ , and  $S_\infty$  of the voltage-dependent activation are defined to be

$$X_\infty(V) = \frac{1}{1 + \exp[(V_X - V)/\theta_X]}, \tag{4}$$

where  $X$  denotes  $M$ ,  $N$ , or  $S$ .

This set of coupled nonlinear differential equations in Eqs. 1 - 3 has been analyzed in detail (35, 36). There it is noted that  $S$  responds on a much slower time scale than  $V$  and  $N$  because  $\tau_S$  has the time scale of several seconds compared with the milli-second time scale in firing. Then  $S$  is regarded just as a parameter, and the dynamics of the fast subsystem on the two-dimensional phase space of  $V$  and  $N$  is analyzed. Furthermore, after eliminating one degree of freedom by substituting  $N_\infty$  to  $N$ , the whole behavior of this model may be analyzed approximately with fast variable  $V$  and slow variable  $S$ .

### Numerical details

Integration of differential equations including noise demands some caution, and is commonly achieved via the Euler method. For better efficiency, we employ the Euler method for integrating the noise term, combined with the second-order Runge-Kutta method for other terms. In order to be concrete, we consider the one-variable problem

$$\frac{dx}{dt} = f(x) + \xi(t), \quad (5)$$

where  $f(x(t))$  is a (nonlinear) function of  $x$ , the variable of concern, and  $\xi(t)$  is the white noise with zero mean and delta-function correlations

$$\begin{aligned} \langle \xi(t) \rangle &= 0, \\ \langle \xi(t)\xi(t') \rangle &= 2D\delta(t-t'). \end{aligned} \quad (6)$$

Taking the time step of size  $\Delta t$ , we obtain from the equation of motion the value of  $x$  at time  $t + \Delta t$ :

$$x(t + \Delta t) = x(t) + \frac{f(x(t)) + f(\bar{x})}{2} \Delta t + \xi(t) \Delta t, \quad (7)$$

where  $\bar{x} \equiv x(t) + f(x(t)) \Delta t + \xi(t) \Delta t$  (37). Although there is no guarantee that this algorithm should converge in general, it works fine here since the noise term does not depend on the variable  $x$  (38).

The white noise  $\xi$  of variance  $D$  is produced by the gaussian random numbers with the variance  $\sigma^2$  determined by

$$\langle \xi(t)^2 \rangle = \int_{-\infty}^{\infty} d\xi \frac{1}{\sqrt{2\pi}\sigma} e^{-\xi^2/2\sigma^2} \xi^2 = \frac{2D}{\Delta t}, \quad (8)$$

where the Dirac delta function has been represented by  $\Delta t^{-1}$  within the numerical accuracy. We thus have the relation  $\sigma = \sqrt{2D/\Delta t}$ .

In our simulations, we take  $\Delta t = 1$  ms, which turns out to be small enough, and integrate the set of equations for current balance. This gives the time evolution of the action potential, from which the power spectrum is computed through the use of the fast Fourier transform technique.

## Results and Discussion

### Noise effects

Before explaining the coupling effects, we first probe the role of noise, either the usual (additive) random noise or the (multiplicative) voltage-dependent



one. Comparison of the effects of such noise helps us to understand better the coupling effects.

### Random noise

Among many kinds of noise on the cell membrane, the simplest case is the random noise, which may come from thermal fluctuations (see below). When such random current fluctuations are present on the membrane, the current balance equation in Eq. 1 is generalized to

$$C_M \frac{dV}{dt} = -I_{ion}(V, N, S) - \xi(t), \quad (9)$$

where  $I_{ion}$  represents all the ionic currents on the right-hand side in Eq. 1, and the noise current  $\xi(t)$  satisfies Eq. 6 with the variance denoted by  $D_\xi$ .

Figure 1 exhibits the solution of the set of coupled differential equations in Eqs. 2 and 9 under various strengths of the random noise. It is observed that single  $\beta$ -cells produce various electrical activities according to the value of  $\tau_N$  in Eq. 2, which lies in the narrow range 4 to 11 ms depending on the membrane potential (27). When the time constant  $\tau_N$  of delayed-rectifier  $K^+$  channel activity exceeds 11.0 ms, the  $\beta$ -cell produces regular spiking action potentials in Fig. 1 *A*, while for  $\tau_N$  below 10.0 ms faster repolarization does not allow enough time for the slow variable  $S$  to decrease, yielding bursting action potentials [see Fig. 1 *C*]. In the intermediate regime of  $\tau_N=10.2$  ms, Fig. 1 *B* shows that spiking action potentials are generated but the bursting property is resident. As an appropriate amount of noise comes into play, in particular, the regular spikes in Figs. 1 *A* and *B* and bursts in *C* change

into fast bursts in  $E$ , irregular spikes in  $G$ , or irregular bursts in  $H$  and  $I$ .

To explain these phenomena, we note two thresholds of the slow variable  $S$ : One is the upper threshold above which the membrane potential is falling into the resting potential; the other is the lower threshold above which the membrane potential begins to fire. At the moment that fluctuations take negative values, they may assist the repolarizing membrane potential to remain above the lower threshold before the membrane repolarizes completely and then, depolarizes slowly to the lower threshold. This induces occasionally consecutive firing in Fig. 1  $G$  or even fast bursts in Fig. 1  $E$  for the  $\beta$ -cell in the critical parameter range, i.e.,  $\tau_N=10.2$  ms. Such consecutive firing raises the average membrane potential for a while, compared with the case of regular spikes. Hence the value of  $S_\infty$  becomes large, and consequently  $S$  grows with the delay represented by the time constant  $\tau_S$ . When it goes over the upper threshold, the membrane potential returns to the resting potential. At the same time,  $S_\infty$  now becomes small and  $S$  reduces to the lower threshold. During this period of  $S$  varying from the upper threshold to the lower one, the membrane potential stays in the silent phase. When  $S$  comes to the lower threshold, the membrane potential starts to depolarize and fire. Repetition of these processes simply constitutes the fast bursts. As the noise level is raised further, the slow variable  $S$  may start to increase before it reaches the lower threshold, assisted by the fluctuations taking negative values. Similarly it may start to decrease before it reaches the upper threshold due to positive fluctuations. In consequence, irregular bursts in Figs. 1  $H$  and  $I$  can thus be induced. When fluctuations become sufficiently strong and dominant, such a role of noise, turning on the slow dynamics of

$S$ , is concealed and the membrane potential appears noisy. Here it is notable that under optimal fluctuations, there exists the critical parameter range in which the difference between the upper and lower thresholds is small and the dramatic effect of fast bursts is produced; similar results were obtained in a recent study (12).

It is revealing to examine the power spectra of the obtained action potentials, computed through the use of the fast Fourier transform technique for various noise levels and displayed in Fig. 2. In particular, Figure 2  $B$  manifests that the regular spiking action potential of frequency 2 Hz in the absence of noise has changed into fast bursts containing oscillations of 0.2 Hz and 5 Hz at moderate noise levels.

To characterize the positive/negative role of noise in bursting, we define the bursting tendency according to  $\mathcal{B} \equiv \log[\mathcal{P}(f_B)/\mathcal{P}(0)]$ , where  $\mathcal{P}(f_B)$  is the power spectrum at the bursting frequency  $f_B$  and  $\mathcal{P}(0)$  is the background intensity at 0 Hz. Figure 3 shows the behavior of the bursting tendency  $\mathcal{B}$  with the noise level, manifesting the noise effects on bursting.

Finally, one may ask whether thermal fluctuations known to generate white noise are enough to induce the fast bursts, irregular bursts or spikes, observed in our simulations. In simulations, the variance  $D_\xi$  is taken in the range  $10^{-29} \text{ J}/\Omega \sim 10^{-27} \text{ J}/\Omega$ . In reality, noise currents due to thermal fluctuations can be estimated via the fluctuation-dissipation theorem:  $D_\xi = k_B T/R$ . This gives  $D_\xi \sim 10^{-29} \text{ J}/\Omega$  when  $R$  is taken to be a few giga ohms ( $\text{G}\Omega$ ) or less. Accordingly, thermal fluctuations alone may not be enough to induce irregular spikes or bursts. Nevertheless, it appears possible that thermal fluctuations actually expedite the emergence of fast bursts when

the cell lies in the critical parameter regime.

### Voltage-dependent noise

As another simple type of noise, one can consider the voltage-dependent fluctuations, which are closely related to the channel gating stochasticity (see below). In the presence of such multiplicative noise, the current balance condition in Eq. 1 takes the form

$$C_M \frac{dV}{dt} = -I_{ion}(V, N, S) - \eta(t)(V - V_K), \quad (10)$$

where  $I_{ion}$  also represents all the ionic currents in Eq. 1, and  $\eta(t)$  is the Gaussian white noise, again satisfying Eq. 6 with variance  $D_\eta$ . Solving numerically the coupled differential equations given by Eqs. 2 and 10 at various noise levels with  $\tau_N$  set equal to 11 ms, we obtain the results, which are illustrated in Fig. 4. Note the overall similarity to the case of random (additive) noise shown in Figs. 1 *D* and *G*.

When the voltage-dependent noise stimulates the cell membrane, irregular spikes arise, similarly to the case of random noise, if its amplitude multiplied by the voltage difference ( $V - V_K$ ) is comparable to the amplitude of random noise. In fact, voltage-dependent noise may be regarded simply as the noise weighted more in the active phase of the membrane potential than in the silent phase. When taking negative values, therefore, fluctuations boost firing more effectively in the active phase and contribute less to the erratic evolution of the resting potential in the silent phase. Such voltage-dependent (multiplicative) noise may arise from ion

channel gating stochasticity, since currents through channels depend upon the membrane potential difference. If the number of channels is sufficiently large, the channel stochasticity can be described by a Langevin equation (39, 40, 41). Specifically, the stochasticity of K(ATP) channels has been considered (20). In the expression for the ATP-dependent  $K^+$  current,  $I_{K(ATP)} = g_{K(ATP)}P(V - V_K)$ , the opening ratio  $P$ , which is no more constant, evolves according to

$$\frac{dP}{dt} = \frac{\gamma_1}{\tau_P}(1 - P) - \frac{\gamma_2}{\tau_P}P + \bar{\xi}(t), \quad (11)$$

where  $\gamma_1/\tau_P$  and  $\gamma_2/\tau_P$  represent the rates for a closed channel to switch to the open state and vice versa, respectively. Note that  $\gamma_1$  and  $\gamma_2$  thus determine the equilibrium ratio between the open state and the closed one. Fluctuations in the opening ratio are described by the Gaussian white noise  $\bar{\xi}(t)$  satisfying Eq. 6 with the variance

$$D_{\bar{\xi}} = \frac{\gamma_1(1 - P) + \gamma_2P}{2\tau_P N_{K(ATP)}} \approx \frac{\gamma_1\gamma_2}{\tau_P N_{K(ATP)}(\gamma_1 + \gamma_2)}, \quad (12)$$

where  $N_{K(ATP)}$  is the total number of ATP-dependent  $K^+$  channels in a  $\beta$ -cell (40).

Solving Eq. 11, we obtain that  $P$  fluctuates around the equilibrium value  $P_0$ , taken to be 0.5 in our simulations:  $P(t) = P_0 + \bar{\eta}(t)$ . Here  $\bar{\eta}(t)$  is colored noise, characterized by the variance

$$\langle \bar{\eta}(t)\bar{\eta}(t') \rangle = D_{\bar{\eta}}[\gamma e^{-\gamma|t-t'|} - \gamma e^{-\gamma(t+t')}] \quad (13)$$

with  $\gamma \equiv (\gamma_1 + \gamma_2)/\tau_p$  and  $D_{\bar{\eta}} \equiv D_{\bar{\xi}}/\gamma^2$  (see Appendix for details). Note that the firing time scale is comparable to the correlation time  $\gamma^{-1}$  of the noise  $\bar{\eta}(t)$  (see Fig. 5). Consequently this colored noise is more effective to induce several consecutive firings, which resemble irregular burst, than the white noise. In particular, the modules of several spikes are observed to become longer as the correlation time  $\gamma^{-1}$  is increased. Figure 6 shows the behaviors in the presence of the channel-gating noise  $\bar{\xi}(t)$  for two different channel numbers. In this case of multiplicative colored noise, modules of spikes arise more efficiently than in the case of mutiplicative white noise shown in Fig. 4. Further, it is also found that stronger gating fluctuations from less channels ( $N_{K(ATP)}=500$ ) in Fig. 6 *B* give rise to modules of more rapid spikes, compared with the case  $N_{K(ATP)}=2500$  in Fig. 6 *A*.

Similar results can be obtained with fluctuations in the  $\text{Ca}^{2+}$  channels and in the delayed-rectifier  $\text{K}^+$  channels although they act somewhat differently from the fluctuations in the ATP-blockable  $\text{K}^+$  channels (data not shown).

It is thus concluded that noise generates diverse firing patterns in single  $\beta$ -cells. In a real (physiological) islet, however,  $\beta$ -cells are not isolated but coupled with each other, making it desirable to consider coupled  $\beta$ -cells and to investigate effects of noise together with those of coupling. This will be the subject of the next section.

### Coupling effects

We consider two cells coupled with each other via a gap junction. With the coupling incorporated, Eq. 1 is extended to the coupled equations:

$$\begin{aligned} C_M \frac{dV_1}{dt} &= -I_{ion}(V_1, N_1, S_1, P_1) - g_C(V_1 - V_2) \\ C_M \frac{dV_2}{dt} &= -I_{ion}(V_2, N_2, S_2, P_2) - g_C(V_2 - V_1), \end{aligned} \quad (14)$$

where the subscripts 1 and 2 are the cell indices,  $I_{ion}$  again denotes all the ionic currents, and  $g_C$  is the coupling conductance. Note that the heterogeneity between both cells is accommodated in the K(ATP) channel opening ratio  $P$ . Namely, the noise associated with channel gating stochasticity induces continuously heterogeneity between the cells.

We thus have eight coupled differential equations, which consist of Eqs. 2 and 11 for each cell and Eq. 14, for eight variables ( $V, N, S$ , and  $P$  for each cell). Integration of these coupled equations yields the results displayed in Fig. 7, for the channel-gating noise of variance  $D_{\xi} = 4 \times 10^{-4} \text{ s}^{-1}$  given by Eq. 12 and for three values of the coupling conductance:  $g_C = 50 \text{ pS}$ ,  $110 \text{ pS}$ , and  $200 \text{ pS}$ . Revealed is the optimal coupling strength for longer bursting periods: While weak coupling is not enough to couple individual cells and to generate consecutive firing, too strong coupling tends to make the cluster behave as a single large cell (22).

Robust bursts emerge as a consequence of the competition between heterogeneity and coupling (23). On one hand, the coupling term in Eq. 14 helps the two cells to act synchronously; on the other hand, it also plays the role

of stimulating noise, which acts strongly on the two cells with asynchronous phases. The perfect asynchrony results from the harmony of coupling to be similar and heterogeneity to be different (see Fig. 8). Namely, the coupling currents between asynchronous neighboring cells give rise to consecutive firing; this in turn increases the upper threshold of the slow variable  $S$  above which firing disappears. As  $S$  grows up toward the increased upper threshold, it takes longer to reduce down to the lower threshold. This larger rising and falling divides more clearly the active and silent phases in the membrane potential, and accordingly induces robust bursting action potentials with periods longer than 20 s. Note that in the absence of coupling we have not been able to observe bursting periods longer than 10 s (see Figs. 1-6) (Parameter values different from those in Table I may yield bursting periods somewhat longer than 10s even in a single cell. In this case, the coupling gives rise to robust bursting of even longer periods, say, 30 s, still demonstrating its crucial role in generating regular bursts.)

In the two-cell model here the optimal value of the coupling conductance is observed to be  $g_C = 110$  pS. As the number of cells is increased, however, more heterogeneity is introduced, which should be matched by stronger coupling to generate robust bursts with longer periods. Although the detailed investigation is beyond our computing capacity, we have performed multi-cell simulations, which indeed confirms such an increase of the optimal coupling conductance. For example, the optimal conductance in the system of 1000 cells turns out to be 100 to 300 pS (data not shown), which coincides with experimental results of the gap junctional conductance (42).

These features of the coupled cells do not change much in the presence



of the voltage-dependent noise instead of the channel-gating noise, except that the channel-gating noise is more efficient for robust bursting than the voltage-dependent one, as shown in Fig. 9 for  $D_\eta = 10^{-24} \text{ J}/\Omega \cdot \text{V}^2$  and  $D_{\bar{\xi}} = 0$ . Note also that the coupled cells depicted in Figs. 7 and 9 do not burst in the absence of noise-induced heterogeneity.

Recall that in the emergence of robust bursts, the asynchrony from the heterogeneity induced by noise plays an important role, which has also been addressed in a very recent study (43). Similar to such noise-induced heterogeneity, the cell-to-cell heterogeneity associated with variations of the cell parameters among the cells is also expected to play for robust bursts (21). To check this, we allowed variations of the membrane capacitance  $C_M$  related to the cell size as well as of the channel conductance  $g_{K(ATP)}$  and examine the resulting behavior: Shown in Fig. 10 *A* and *B* are bursts generated in the case of 20% variation of  $C_M$  (5.0 pF, 6.3 pF) and in the case of 10% variation of  $g_{K(ATP)}$  (1000 pS, 1100 pS), respectively. Specifically, a spiking cell (with  $C_M = 6.3 \text{ pF}$ ) is coupled with a bursting cell (with  $C_M = 5.0 \text{ pF}$ ) in Fig. 10 *A*, which results in that both cells are bursting synchronously with a longer bursting period than that of a single cell (5.0 pF). In Fig. 10 *B*, on the other hand, two spiking cells (with  $g_{K(ATP)} = 1000 \text{ pS}$  and  $1100 \text{ pS}$ ) are coupled with each other, and both are bursting. Therefore heterogeneity is in general important for bursting in coupled cells, no matter whether it is cell-to-cell heterogeneity or induced by noise.

## Conclusions

We have probed whether noise and coupling serve as an appropriate stimulus for inducing the bursting action potential in pancreatic  $\beta$ -cells, and found that they effectively call into action the inherent slow dynamics in individual cells. Fast bursts, irregular spikes or bursts in single  $\beta$ -cells have been observed as the results of the noise effects. In particular the emergence of regular bursts assisted by an appropriate amount of noise [see Figs. 1 *E* and 2 *B*] is reminiscent of *coherence resonance* (15, 16, 17, 18, 19). In view of physiology, the consecutive firing induced by fluctuations gives rise to relative depolarization for a while, which is followed by the activation of the slow potassium channel lasting until the slow variable reaches the upper threshold. At this time the slow  $K^+$  channel opens fully, and the outflux of cytosolic potassium ions gets very large, thus hindering depolarization. Accordingly, the membrane potential is compelled to stay in the silent phase, and the slow  $K^+$  channel in turn starts to be inactivated. In consequence, the membrane can become depolarized as the outflux of  $K^+$  ions reduces. Finally, firing occurs again, and consecutive firing also happens by the help of appropriate stimulation. As candidates for the stimulus, both the (additive) random noise coming from fluctuating currents and the (multiplicative) voltage-dependent noise from the channel gating stochasticity have been considered.

In particular, coupling between cells has turned out essential for attaining regular bursts with longer periods compared with the fast bursts. The coupling term, proportional to the potential difference between two cells,

operates in a similar manner to the voltage-dependent noise: It increases with the potential difference and thus becomes large for the cells in active phases, stimulating the cells like noise. On the other hand, it is small for perfectly synchronized cells in silent phases. The coupling also increases the upper threshold of  $S$  and induces robust regular bursts.

In the analysis, the heterogeneity has been found to play an important role in inducing strong fluctuations during active phases, which may cause robust bursts. Namely, bursting in general results from the interplay of coupling and heterogeneity. This allows us to interpret the fact that large cell clusters (up to the critical size) show more regular bursts (20, 22): Assuming a cubic islet, we have considered  $\beta$ -cells arranged into an  $L^3$  cube, under free boundary conditions. Adopting physiological gap junction conductance,  $g_C = 200$  pS (42), we have found that the bursting period and duration first increases with the size  $L$  but tends to saturate beyond  $L = 5$  (data not shown). Such saturation behavior may be explained as follows: Via the coupling through gap junctions, the number of nearest neighbors in the three-dimensional space is limited, e.g., to six or so; this suggests that the cluster above some critical size can get no more advantage of the heterogeneity from neighboring cells through given coupling strength.

The Langerhans islet, however, consists of several endocrine cells in addition to  $\beta$ -cells. Other endocrine cells in an islet have been studied recently (44, 45), and it will be of interest to study the coupling effects between originally different  $\alpha$ -,  $\beta$ -, and  $\delta$ -cells, coupled via hormones or neurotransmitters (46). This might give a clue to understanding the size of a Langerhans islet in the pancreas, which is left for further study.

## Appendix

Equation 11 can be solved to give the time evolution of the opening ratio  $P$ :

$$P(t) = P_0 + [P(0) - P_0]e^{-\gamma t} + \int_0^t e^{-\gamma(t-t')} \bar{\xi}(t') dt'$$

with  $P_0 \equiv \gamma_1/(\gamma_1 + \gamma_2)$  and  $\gamma \equiv (\gamma_1 + \gamma_2)/\tau_p$ , where  $P(0)$  is the initial value of  $P$ . After sufficiently long time, we thus have  $P$  fluctuating around the equilibrium ratio  $P_0$ :  $P(t) = P_0 + \bar{\eta}(t)$ , where the noise  $\bar{\eta}(t)$  is given by

$$\bar{\eta}(t) \equiv \int_0^t e^{-\gamma(t-t')} \bar{\xi}(t') dt'.$$

From the above definition of the noise  $\bar{\eta}(t)$ , it is straightforward to derive its characteristics:

$$\begin{aligned} \langle \bar{\eta}(t) \bar{\eta}(t') \rangle &= \int_0^t d\tau e^{\gamma(\tau-t)} \int_0^{t'} d\tau' e^{\gamma(\tau'-t')} \langle \bar{\xi}(\tau) \bar{\xi}(\tau') \rangle \\ &= 2D_{\bar{\xi}} e^{-\gamma(t+t')} \int_0^{\bar{t}} d\tau e^{2\gamma\tau}, \end{aligned}$$

where we have used the relation  $\langle \bar{\xi}(\tau) \bar{\xi}(\tau') \rangle = 2D_{\bar{\xi}} \delta(\tau - \tau')$  and  $\bar{t}$  denotes the smaller one between  $t$  and  $t'$ . We thus obtain the correlations of the noise  $\bar{\eta}$  at different times

$$\langle \bar{\eta}(t) \bar{\eta}(t') \rangle = D_{\bar{\eta}} [\gamma e^{-\gamma|t-t'|} - \gamma e^{-\gamma(t+t')}]$$

with  $D_{\bar{\eta}} \equiv D_{\bar{\xi}}/\gamma^2$ , which manifests the colored nature.

This work was supported in part by KOSEF through Grant No. 01-2002-000-00285-0 and by the MOST (KOSEF) through National Core Research Center for Systems Bio-Dynamics, as well as by the BK21 Program. Helpful reprints from the Laboratory of Biological Modeling in NIDDK of NIH are also gratefully acknowledged.

## References

1. Falke, L. C., K. D. Gillis, D. M. Pressel, and S. Mislner. 1989. 'Perforated patch recording' allows long-term monitoring of metabolite-induced electrical activity and voltage-dependent  $\text{Ca}^{2+}$  currents in pancreatic islet  $\beta$ -cells. *FEBS Lett.* 251:167–172.
2. Kinard, T. A., G. de Vries, A. Sherman, and L. S. Satin. 1999. Modulation of the bursting properties of single mouse pancreatic  $\beta$ -cells by artificial conductances. *Biophys. J.* 76:1423–1435.
3. Smith, P. A., F. M. Ashcroft, and P. Rorsman. 1990. Simultaneous recordings of glucose dependent electrical activity and atp-regulated  $\text{K}^{+}$ -currents in isolated mouse pancreatic  $\beta$ -cells. *FEBS Lett.* 261:187–190.
4. Andreu, E., B. Soria, and J. V. Sánchez-Andrés. 1997. Oscillation of gap junction electrical coupling in the mouse pancreatic islets of langerhans. *J. Physiol.* 498:753–761.
5. Dean, P. M., and E. K. Matthews. 1968. Electrical activity in pancreatic islet cells. *Nature* 219:389–390.

6. Sánchez-Andrés, J. V., A. Gomis, and M. Valdeolmillos. 1995. The electrical activity of mouse pancreatic  $\beta$ -cells recorded in vivo shows glucose-dependent oscillations. *J. Physiol.* 486:223–228.
7. Valdeolmillos, M., A. Gomis, and J. V. Sánchez-Andrés. 1996. In vivo synchronous membrane potential oscillations in mouse pancreatic  $\beta$ -cells: lack of co-ordination between islets. *J. Physiol.* 493:9–18.
8. Henquin, J. C., and H. P. Meissner. 1984. Significance of ionic fluxes and changes in membrane potential for stimulus-secretion coupling in pancreatic  $\beta$ -cells. *Experientia* 40:1043–1052.
9. Bosco, D., L. Orci, and P. Meda. 1989. Homologous but not heterologous contact increases the insulin secretion of individual pancreatic  $\beta$ -cells. *Exp. Cell Res.* 184:72–80.
10. Halban, P. A., C. B. Wollheim, B. Blondel, P. Meda, E. N. Niesor, and D. H. Mintz. 1982. The possible importance of contact between pancreatic islet cells for the control of insulin release. *Endocrinology* 111:86–94.
11. Pipeleers, D., P. I. Veld, E. Maes, and M. V. D. Winkel. 1982. Glucose-induced insulin release depends on functional cooperation between islet cells. *Proc. Natl. Acad. Sci. USA* 79:7322–7325.
12. Aguirre, J., E. Mosekilde, and M. A. F. Sanjuán. 2004. Analysis of the noise-induced bursting-spiking transition in a pancreatic  $\beta$ -cell model. *Phys. Rev. E* 69:041910.

13. Chay, T. R., and H. S. Kang. 1988. Role of single-channel stochastic noise on bursting clusters of pancreatic  $\beta$ -cells. *Biophys. J.* 54:427–435.
14. Sherman, A., J. Rinzel, and J. Keizer. 1988. Emergence of organized bursting in clusters of pancreatic  $\beta$ -cells by channel sharing. *Biophys. J.* 54:411–425.
15. Lee, S. G., A. Neiman, and S. Kim. 1998. Coherence resonance in a hodgkin-huxley neuron. *Phys. Rev. E* 57:3292–3297.
16. Longtin, A. 1997. Autonomous stochastic resonance in bursting neurons. *Phys. Rev. E* 55:868–876.
17. Pei, X., L. Wilkens, and F. Moss. 1996. Noise-mediated spike timing precision from aperiodic stimuli in an array of hodgkin-huxley-type neuron. *Phys. Rev. Lett.* 77:4679–4682.
18. Pikovsky, A. S., and J. Kurths. 1997. Coherence resonance in a noise-driven excitable system. *Phys. Rev. Lett.* 78:775–778.
19. Zaikin, A., J. García-Ojalvo, R. Báscones, E. Ullner, and J. Kurths. 2003. Doubly stochastic coherence via noise-induced symmetry in bistable neural models. *Phys. Rev. Lett.* 90:03061.
20. de Vries, G., and A. Sherman. 2000. Channel sharing in pancreatic  $\beta$ -cells revisited: enhancement of emergent bursting by noise. *J. Theor. Biol.* 207:513–530.
21. Smolen, P., J. Rinzel, and A. Sherman. 1993. Why pancreatic islets burst

- but single beta cells do not. the heterogeneity hypothesis. *Biophys. J.* 64:1668–1680.
22. Sherman, A., and J. Rinzel. 1991. Model for synchronization of pancreatic  $\beta$ -cells by gap junction coupling. *Biophys. J.* 59:547–559.
  23. de Vries, G., and A. Sherman. 2001. From spikers to bursters via coupling: help from heterogeneity. *Bull. Math. Biol.* 63:371–391.
  24. Sherman, A., and J. Rinzel. 1992. Rhythmogenic effects of weak electrotonic coupling in neuronal models. *Proc. Natl. Acad. Sci. USA* 89:2471–2474.
  25. Hodgkin, A. L., and A. F. Huxley. 1952. A quantitative description of membrane current and its application to conduction and excitation in nerve. *J. Physiol.* 117:500–544.
  26. Ashcroft, F. M., and P. Rorsman. 1989. Electrophysiology of the pancreatic  $\beta$ -cell. *Prog. Biophys. Mol. Biol.* 54:87–143.
  27. Göpel, S., T. Kanno, S. Barg, J. Galvanovskis, and P. Rorsman. 1999. Voltage-gated and resting membrane currents recorded from  $\beta$ -cells in intact mouse pancreatic islets. *J. Physiol.* 521:717–728.
  28. Rorsman, P., and G. Trube. 1986. Calcium and delayed potassium currents in mouse pancreatic  $\beta$ -cells under voltage-clamp conditions. *J. Physiol.* 374:531–550.
  29. de Vries, G. 2001. Bursting as an emergent phenomenon in coupled chaotic maps. *Phys. Rev. E* 64:051914.



30. Rulkov, N. F. 2001. Regularization of synchronized chaotic bursts. *Phys. Rev. Lett.* 86:183–186.
31. Rulkov, N. F. 2002. Modeling of spiking-bursting neural behavior using two-dimensional map. *Phys. Rev. E* 65:041922.
32. Sherman, A. 1996. Contributions of modeling to understanding stimulus-secretion coupling in pancreatic  $\beta$ -cells. *Am. J. Physiol.* 271:362–372.
33. Chay, T. R., and J. Keizer. 1983. Minimal model for membrane oscillations in the pancreatic beta-cell. *Biophys. J.* 42:181–190.
34. Keizer, J., and G. Magnus. 1989. ATP-sensitive potassium channel and bursting in the pancreatic beta cell. a theoretical study. *Biophys. J.* 56:229–242.
35. Keener, J., and J. Sneyd. 1998. *Mathematical Physiology*. Springer-Verlag, New York, 188–215.
36. Rinzel, J. 1987. A formal classification of bursting mechanisms in excitable systems. *In* *Mathematical Topics in Population Biology, Morphogenesis, and Neurosciences*, E. Teramoto, and M. Yamaguti, editors. Springer-Verlag, New York, 267–281.
37. Batrouni, G. G., G. R. Katz, A. S. Kronfeld, G. P. Lepage, B. Svetitsky, and K. G. Wilson. 1985. Langevin simulations of lattice field theories. *Phys. Rev. D* 32:2736.

38. Kloeden, P. E., E. Platen, and H. Schurz. 1994. Numerical Solution of SDE through Computer Experiments. Springer-Verlag, Berlin, 151.
39. DeFelice, L. J., and A. Isaac. 1992. Chaotic states in a random world: relationship between the nonlinear differential equations of excitability and the stochastic properties of ion channels. *J. Stat. Phys.* 70:339–354.
40. Fox, R. F., and Y. N. Lu. 1994. Emergent collective behavior in large numbers of globally coupled independently stochastic ion channels. *Phys. Rev. E* 49:3421–3431.
41. Fox, R. F. 1997. Stochastic versions of the hodgkin-huxley equations. *Biophys. J.* 72:2068–2074.
42. Pérez-Armendariz, M., C. Roy, D. C. Sparay, and M. V. L. Bennett. 1991. Biophysical properties of gap junctions between freshly dispersed pairs of mouse pancreatic beta cells. *Biophys. J.* 59:76–92.
43. Pedersen, M. G. 2005. A comment on noise enhanced bursting in pancreatic  $\beta$ -cells. *J. Theor. Biol.* 235:1–3.
44. Kanno, T., S. O. Göpel, P. Rorsman, and M. Wakui. 2002. Cellular function in multicellular system for hormone-secretion: electrophysiological aspect of studies on  $\alpha$ -,  $\beta$ - and  $\delta$ -cells of the pancreatic islet. *Neurosci. Res.* 42:79–90.
45. Nadal, A., I. Quesada, and B. Soria. 1999. Homologous and heterologous asynchronicity between identified alpha-, beta- and delta-cells within intact islets of langerhans in the mouse. *J. Physiol.* 517:85–93.

46. Moriyama, Y., and M. Hayashi. 2003. Glutamate-mediated signaling in the islets of langerhans: a thread entangled. *TRENDS in Pharmacol. Sci.* 42:511–517.

**Table**

Table 1: Standard parameter values

$C_M = 6.3$ pF	$g_{Ca} = 3000$ pS
$g_K = 4000$ pS	$g_{K(ATP)} = 1000$ pS
$g_S = 3000$ pS	$g_C = 110$ pS
$V_{Ca} = 25$ mV	$V_K = -75$ mV
$V_M = -20$ mV	$\theta_M = 12$ mV
$V_N = -17$ mV	$\theta_N = 5.6$ mV
$V_S = -22$ mV	$\theta_S = 8.0$ mV
$\tau_N = 1.1 \times 10^{-2}$ s	$\tau_S = 20$ s
$\tau_P = 0.50$ s	$N_{K(ATP)} = 2500$
$\gamma_1 = 1$	$\gamma_2 = 1$

## Figure Legends

### Figure 1.

Action potential  $V$  and slow channel activity  $S$  in single  $\beta$ -cells at the noise level  $D_\xi = 0, 10^{-29}$ , and  $10^{-27}$  J/ $\Omega$  under several values of time constant  $\tau_N$  of delayed-rectifier  $K^+$  channel activity  $N$ . All simulations have been performed under the standard parameter values in Table I except  $\tau_N$ , the values of which are given above.

### Figure 2.

Power spectra of the action potentials for the random noise levels in Fig. 1. The time constant  $\tau_N$  of the activation variable  $N$  is (A) 11.0 ms and (B) 10.2 ms. Observed in the power spectra are main peaks together with their harmonics. The peak at 1 Hz, indicated by the asterisk in (B), reflects the tendency to form dimerization of spikes. Each power spectrum has been obtained from the average over 1000 samples, each having a time sequence of 132 seconds.

### Figure 3.

Bursting tendency  $\mathcal{B}$  of  $\beta$ -cells versus the noise level for several values of  $\tau_N$ , corresponding to different firing patterns in the absence of noise.

### Figure 4.

Action potential  $V$  and slow channel activity  $S$  in single  $\beta$ -cells at two values of the voltage-dependent noise. Again parameter values in Table I have been

used.

**Figure 5.**

Correlations between the action potential and multiplicative colored noise due to channel-gating stochasticity. The correlation time  $\gamma^{-1}$  is taken to be (A) 25 ms, (B) 250 ms, and (C) 2500 ms. Note that each figure has a different time scale. Their corresponding power spectra are shown in (D). Parameter values in Table I have been used except  $\tau_P$ .

**Figure 6.**

Action potential  $V$  and slow channel activity  $S$  in single  $\beta$ -cells at two values of the channel gating stochasticity: (A) and (B) correspond to the channel number  $N_{K(ATP)} = 2500$  and 500, respectively. Note that Figs. 5 B and 6 A represent the same sample path, but with different variables plotted. Other parameter values have been taken from Table I.

**Figure 7.**

Figure 8. Enlarged view of the interval between 10 s to 11 s in Fig. 7 B, disclosing the detailed behavior of the two membrane potentials  $V_1$  (*solid line*) and  $V_2$  (*dashed line*).

**Figure 9.**

Bursting action potential induced by cell coupling via the gap junction of conductance  $g_C = 110$  pS under the voltage-dependent noise of strength  $D_\eta = 10^{-24}$  J/ $\Omega \cdot V^2$ . Parameter values in Table I have been used.

**Figure 10.**

Bursting action potential induced by cell coupling, with the cell-to-cell heterogeneity due to variations of the membrane capacitance  $C_M$  and of the ATP-blockable  $K^+$  channel conductance  $g_{K(ATP)}$ : (A) 20 % variation of  $C_M$  (5.0 pF, 6.3 pF); (B) 10 % variation of  $g_{K(ATP)}$  (1000 pS, 1100 pS). Other parameter values have been taken from Table I.

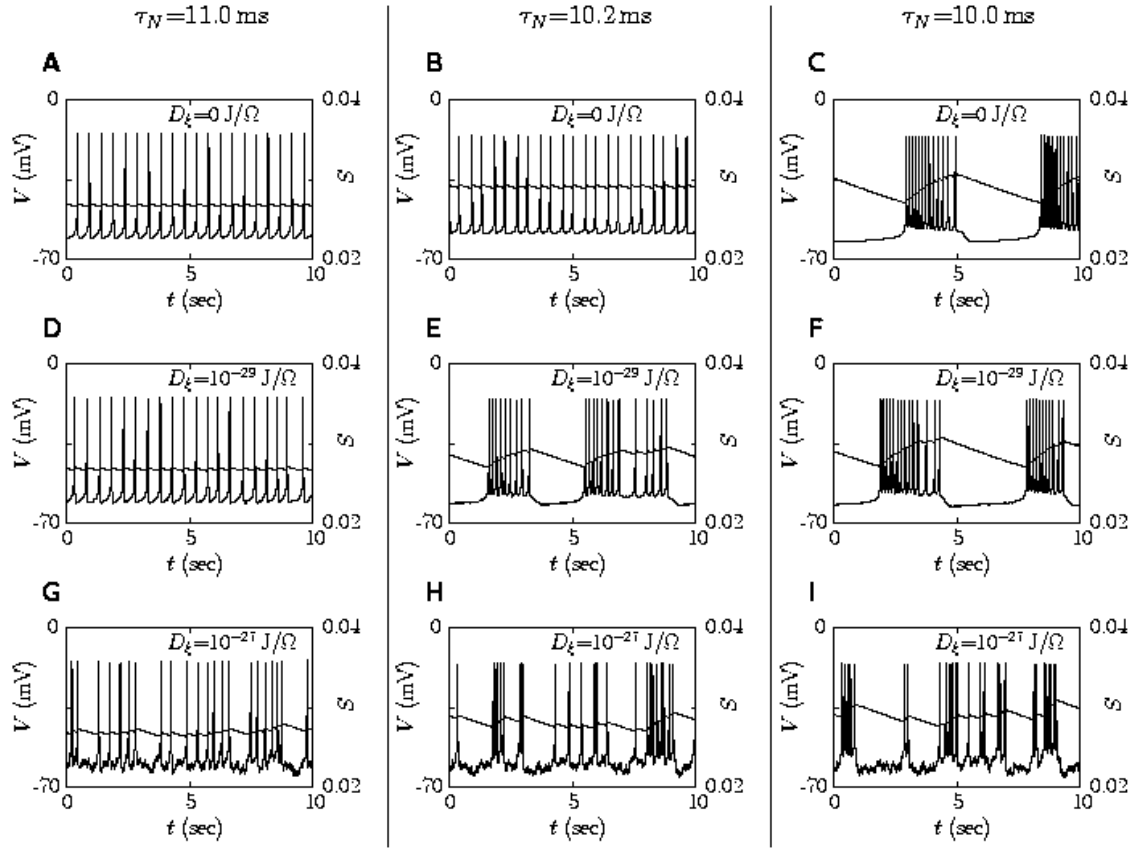


Figure 1:



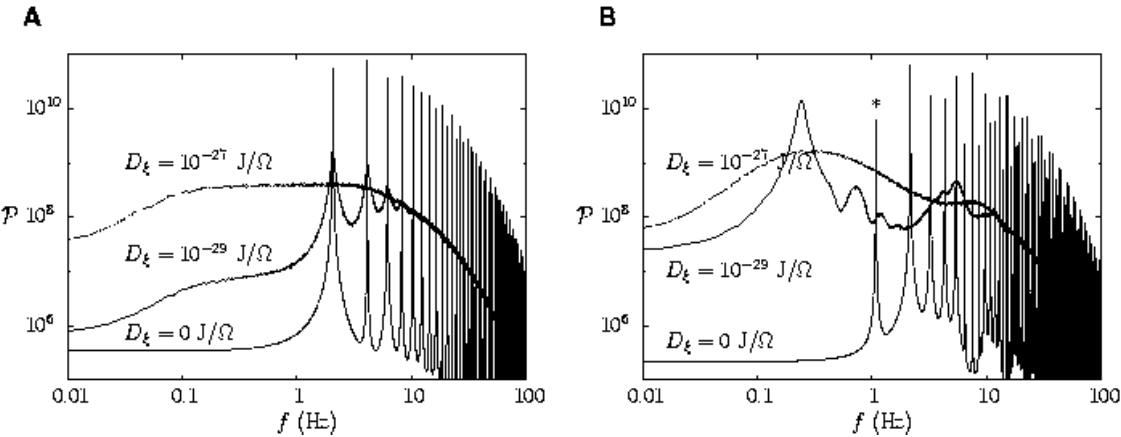


Figure 2:

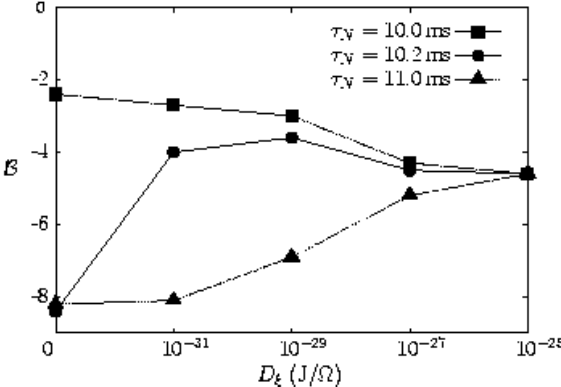


Figure 3:

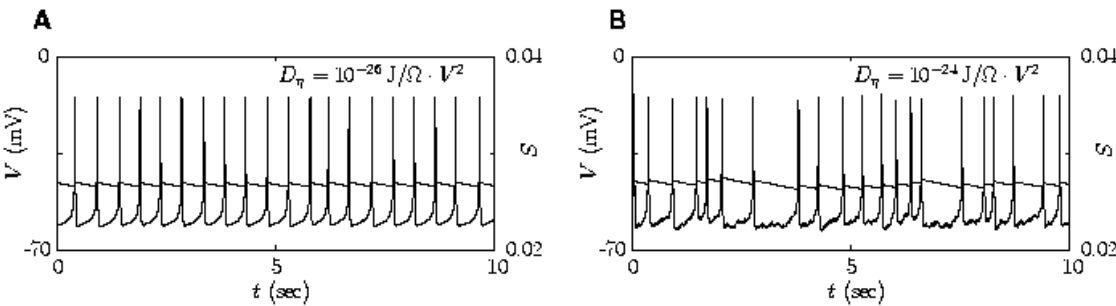


Figure 4:

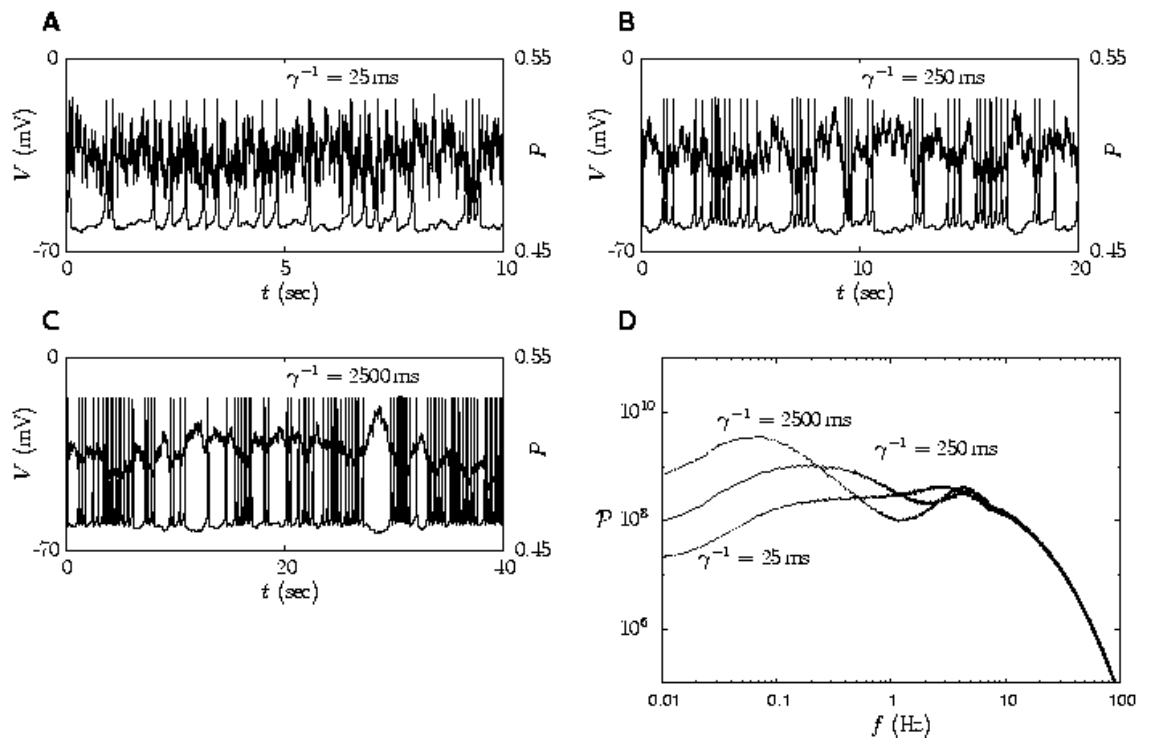


Figure 5:

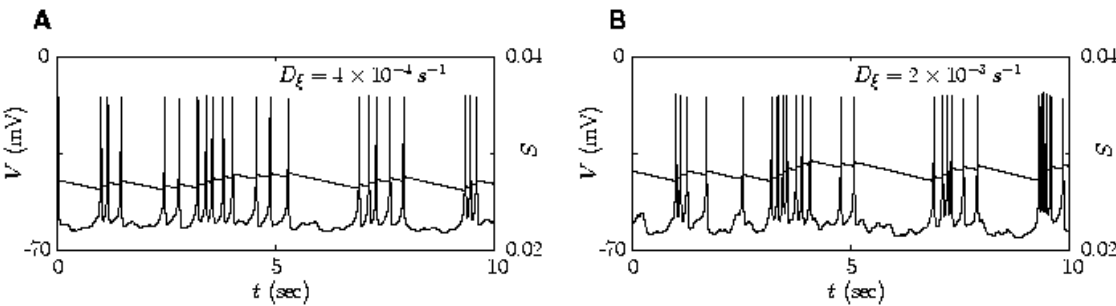


Figure 6:

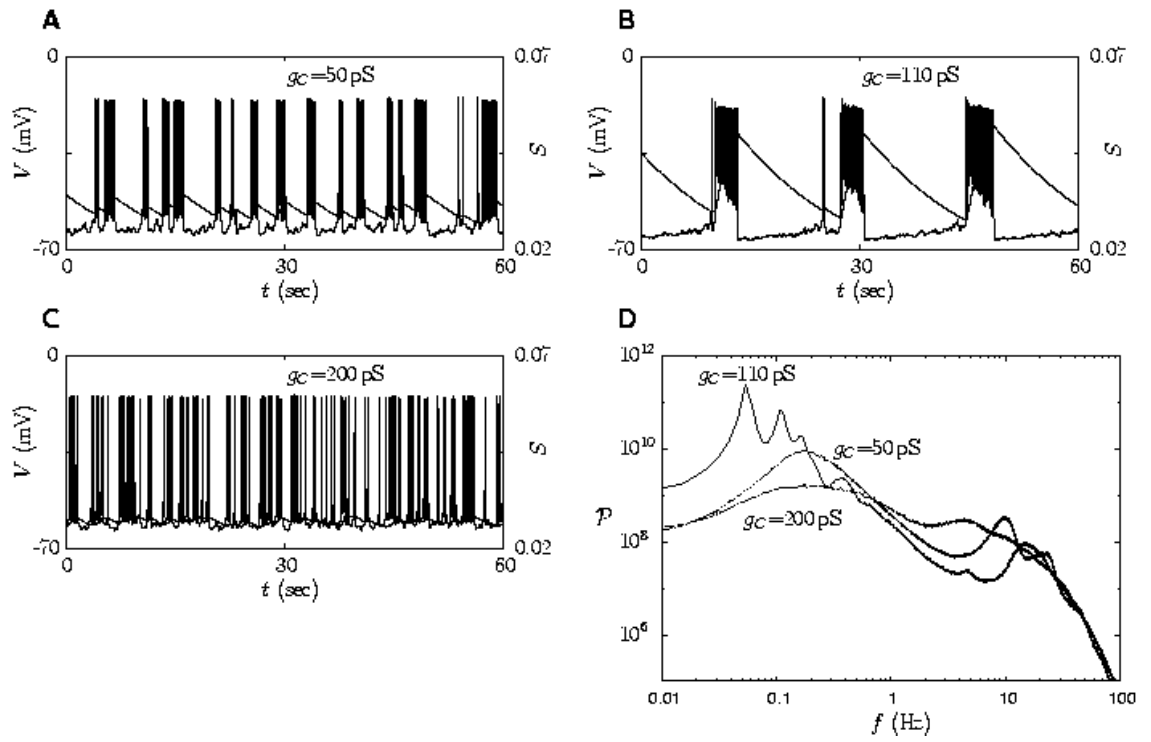


Figure 7:

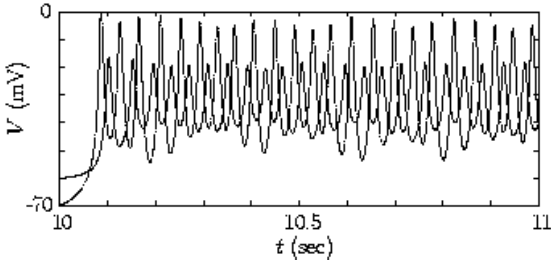


Figure 8:

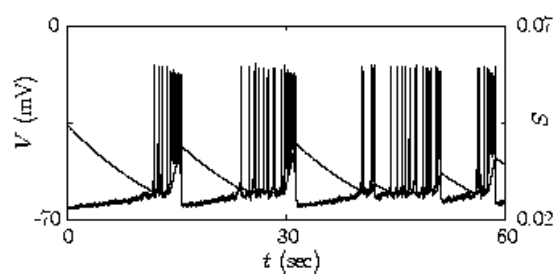


Figure 9:



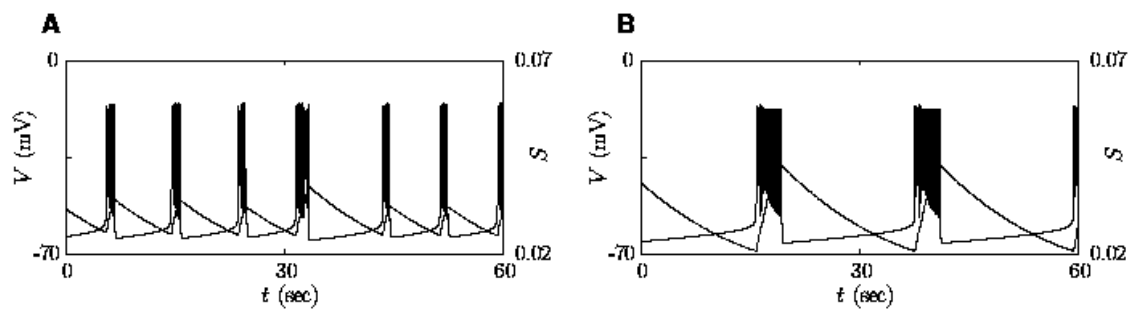


Figure 10: